

Preparation of zinc containing materials

Mohammad Afzaal, Mohammad A. Malik and Paul O'Brien*

Received (in Montpellier, France) 8th August 2007, Accepted 22nd October 2007

First published as an Advance Article on the web 1st November 2007

DOI: 10.1039/b712235g

There has been an immense recent interest in zinc oxide and chalcogenide materials because of their potential use in many devices. The synthesis and characterisation of ZnE (E = O, S, Se and Te) thin films or types of quantum dots has as a consequence become topical. A close interplay between the development of new or improved synthetic methods and the resulting material properties has evolved.

1 Introduction

Zinc containing materials, particularly oxides and chalcogenides, have been under investigation for many years. In the last two decades, new developments in processing and characterization techniques have led to a better understanding of the chemical, physical and optical properties of such materials and consequently have opened new technologies for device construction. Table 1 gives the properties of some zinc containing materials.¹

Zinc sulfide (ZnS) is a direct wide band gap semiconductor with a high index of refraction and good transmittance in the visible range. It is one of the most important materials in photonics research.^{2,3} When it is doped with elements such as Eu and Tb, a wide range of exciting optical properties can be evolved.⁴ Quantum dots especially core-shell structures such as CdSe/ZnS have been found to exhibit lasing effects and can be used in fluoro-immunoassays, biological imaging and biosensors.^{5,6} In the bulk state, ZnS typically exists as the zinc blende (cubic) form at room temperature. At elevated temperatures, bulk ZnS can undergo a phase transformation from the cubic structure to the hexagonal wurtzitic form.^{7,8} The hexagonal form has more desirable optical properties than the cubic form. This transformation has been shown to occur at 1013 or 1031 °C depending on the activity of sulfur,^{8d} suggest-

ing some link between stability and stoichiometry at higher temperatures. The energetic differences between these two phases are extremely small (2 kJ mol⁻¹),^{8e} which results in the frequent co-existence of the both forms. Another important characteristic of ZnS is its polar surface. The most common polar surface is the basal plane. The oppositely charged ions produce positively charged Zn(0001) and negatively charged S(000 $\bar{1}$) polar surfaces, resulting in a normal dipole moment and polarization along the *c*-axis as well as a divergence in surface energy.⁷

Zinc selenide (ZnSe) and zinc telluride (ZnTe), are narrower band gap semiconductors, and have structures which are closely related to that of ZnS (see Table 1). Because of its band gap, ZnSe has been seen as a material for the fabrication of various optoelectronic devices such as solar cells, light-emitting diodes, and lasers that operate in the blue-green region.⁹⁻¹¹ Zinc telluride is an attractive semiconductor with a direct band gap of 2.28 eV and a Bohr exciton radius of 6.2 nm.¹² It has been suggested as a useful material in optoelectronic and thermoelectric devices, such as; in tandem solar cells, a buffer layer for a HgCdTe infrared detector, or as part of the graded *p*-Zn(Te)Se multiquantum-well structure in a blue-green laser diode.¹³⁻¹⁵

An extensive literature exists detailing the synthesis and properties of zinc oxide (ZnO) thin films and nanostructures. Zinc oxide is a wide band gap material (3.37 eV), with a high exciton binding energy (60 eV), which ensures efficient excitonic ultraviolet (UV) emission at room temperature.¹⁶ The thermodynamically stable phase for ZnO is zincite with the

*The School of Chemistry and The School of Materials, The University of Manchester, Oxford Road, Manchester, UK M13 9PL.
E-mail: paul.obrien@manchester.ac.uk; Fax: 0161-275-4616;
Tel: 0161-275-4652*



Mohammad Afzaal graduated from Aston University, Birmingham in 2000 and moved to University of Manchester to carry out his PhD with Professor Paul O'Brien studying growth of semiconductor thin films using single-source precursors. After completing his PhD in 2003, he remained with Professor Paul O'Brien and took his current post-doctoral position, studying nanoparticles and thin film deposition.



Mohammad Azad Malik has been working with Prof. Paul O'Brien for the last 18 years. He has been involved in various projects and has wide range of experience including single-source molecular precursors for II/VI, III/V and III/VI semiconductors, MOCVD, AACVD, CBD, and the colloidal synthesis of nanoparticles.

Table 1 Properties of some zinc containing semiconductors^a

Compd	Band gap ^a /eV	Type ^b	Structure	Lattice spacing/Å
ZnO	3.37	d	Wurtzite	4.58
ZnS	3.8	d	Wurtzite	<i>a</i> : 3.814; <i>c</i> : 6.257
ZnS	3.6	d	Zinc blende	5.406
ZnSe	2.58	d	Zinc blende	5.667
ZnTe	2.28	d	Zinc blende	6.101

^a At 300 K. ^b d, direct.

wurtzite (hcp) structure. Two cubic phases are known, the sphaleritic (zinc blende)¹⁷ and a high pressure rocksalt form.¹⁸ Polycrystalline thin films of ZnO have been employed in SAW devices, optical waveguides, transparent conducting electrodes and as window layers in chalcopyrite based solar cells.¹⁹ Nanophase ZnO has become of interest as an alternative to the TiO₂ layer in Grätzel-type photocells.²⁰ There has been a lot of interest in doping ZnO with 3d transition metal ions because of potential in spin-based electronics (spintronics). Manganese-doped ZnO has been shown to be ferromagnetic at room temperature²¹ and studies on bulk and nanocrystalline ZnO doped with transition metal ions are primarily concerned with the magnetic properties and/or magnetic applications.²² Current work has focused on ZnO/ZnS and ZnO/ZnTe heterostructures and their exploitation in photovoltaic applications by tuning their optical properties.²³

This review will highlight recent advances in methods for preparing zinc oxide or chalcogenides, as thin films and nanomaterials, with particular emphasis on results from our laboratory.

2 Vapor phase deposition of zinc chalcogenide thin films

2.1 Conventional approach

The deposition of thin films from the gas phase can be carried out by many different methods mainly belonging to two

families: physical and chemical vapor deposition (PVD, CVD). Both methods use physical transport of the vapor species to the deposition site. Deposition techniques belonging to PVD family such as evaporation or sputtering processes have been used for the growth of ZnE (E = S, Se, Te)^{24–26} and ZnO^{27,28} thin films. The deposition of ZnE (E = S, Se, Te) thin films by CVD techniques has been widely studied. The first reports of ZnS by MOCVD used diethylzinc (Et₂Zn) in the presence of hydrogen sulfide (H₂S).²⁹ Although good quality thin films of, for example ZnSe, with excellent electrical and optical properties have been obtained at low substrate temperature (~300 °C) a severe premature reaction frequently occurs in the gas phase. The premature reaction during ZnS or ZnSe growth can be attributed to the facile elimination of alkyl groups from R₂Zn by acidic hydrogen from H₂Se or H₂S. Much effort has therefore gone into developing alternative precursors which are less likely to undergo such parasitic reactions.

One alternative approach has been to modify the zinc precursor so that it will be less volatile. For instance, the adducts [Me₂Zn(1,4-dioxane)] and [Me₂Zn(1,4-thioxane)] have been shown to reduce prereaction with H₂Se, while still allowing the growth of ZnSe at low temperature (200–350 °C).³⁰ A significant advance was achieved by the use of a nitrogen donor adduct, dimethylzinc triethylamine [(Me₂Zn)(NEt₃)], as a precursor for ZnS or ZnSe.³¹ There are a number of significant advantages associated with its use.³² Firstly, the premature reaction with H₂Se or H₂S is eliminated rather than merely inhibited. Secondly, [(Me₂Zn)(NEt₃)] is not pyrophoric and is less susceptible to contamination by oxygen containing impurities (*e.g.*, (MeO)ZnMe). [(Me₂Zn)(NEt₃)] is also much easier to purify than Me₂Zn. Finally, it has been shown that [(Me₂Zn)(NEt₃)] forms a eutectic mixture, leading to a more reproducible delivery of the precursor (Fig. 1).³³

Both (Et₂Zn) and (Me₂Zn) have been used to p-dope GaAs and InP.^{34–36} There are, however, problems associated with their use. For instance, (Et₂Zn) has a relatively low thermal stability and light sensitive, which makes it difficult to manufacture in pure form and also leads to zinc depletion from the gas phase, adversely affecting doping uniformity. Therefore, adducts such as [(Me₂Zn)(NEt₃)] are now used for



Paul O'Brien has been Professor of Inorganic Materials Chemistry in the School of Chemistry and the School of Materials at University of Manchester since 1999 and is at present Head of the School of Chemistry. He was Research Dean in the Faculty of Science and Engineering at University of Manchester from 2001–2003 and in 2002, he founded Nanoco Ltd, to commercialize quantum dot

synthesis. In 2001, he received the Potts Medal (distinguished alumnus award University of Liverpool) and in 2005 he gave the A. G. Evans Memorial Medal lecture at Cardiff University. In 2006 he was awarded the first honorary DSc degree from the University of Zululand, South Africa and in 2007 is the Kroll medallist of IOMMM.

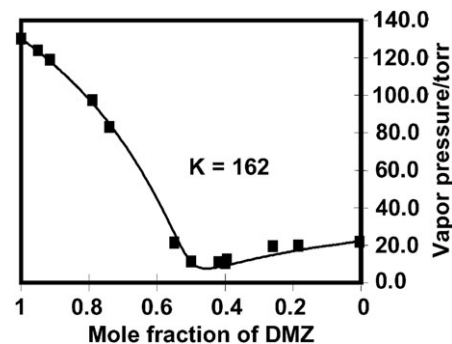


Fig. 1 Eutectic behavior of mixtures of Me₂Zn and Et₃N, showing a minimum between *x* = 0.4 and *x* = 0.6, characteristic of the formation of a weak adduct.

reproducible doping of InP and GaAs.³⁷ The p-doped InP and InGaAs layers had excellent surface morphology with no detrimental prereaction being evident. It was also noted that the major advantages of using [(Me₂Zn)(NEt₃)] are its purity, ease of handling, long term stability and improved reproducibility from batch to batch as compared with Me₂Zn–H₂ gas mixtures.

2.2 Single-source precursors

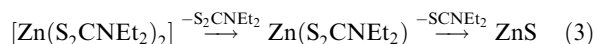
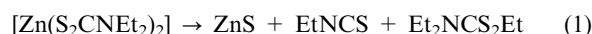
In order to reduce toxic hazards, elimination of homogenous prereaction and lower deposition temperatures, considerable effort has been directed toward the development of alternative precursors for use in MOCVD. One approach is to use a single-source precursor, in which all the elements required in the film are present in a single molecule.

Thiolato and the other chalcogenolato complexes of zinc and cadmium are the simplest candidates as single-source precursors of zinc or cadmium chalcogenides. The solid-state chemistry of cadmium and zinc with the chalcogens is typified by the formation of polymeric structures often with tetrahedral metal ion coordination.³⁸ The adamantyl structures of many thiolates with zinc and cadmium provide well-characterised examples of such behaviour,^{39–41} as do the polymeric chain complexes formed by pyridinethione and 2,3-mercaptobenzothiazole with cadmium and zinc.^{42,43} Bochmann *et al.* have extended such chemistry by synthesizing a range of precursors based on 2,4,6-tri-*tert*-butylphenylchalcogenolates, and these have been used to deposit thin films of the metal sulfides and selenides in preliminary low-pressure growth experiments.^{44–46} One problem with such ligands is that steric bulk is achieved by the incorporation of large number of aryl-carbon atoms and carbon incorporation into thin films grown from such precursors is a distinct possibility. Another series of precursors involve silicon based systems of stoichiometry [(M)Si(SiCH₃)₃]₂ (M = Zn, Cd, Hg; E = S, Se or Te).^{47,48} Thin films of the tellurides having been deposited by low-pressure MOCVD.⁴⁹

Thiophosphinato complexes are yet another class of chalcogen containing compounds that may be useful as precursors. Takahashi *et al.*⁵⁰ deposited cadmium and zinc sulfides using methylthiophosphinates [M(S₂PMe₂)₂] (M = Cd, Zn). However, the use of compounds containing a phosphorus moiety as in the thiophosphinato ligand is undesirable: CdS shows normally n-type conduction, due to non-stoichiometry, and doping with phosphorus would lead to highly compensated semi-insulating material.

Dithiocarbamate complexes are another potential candidate as precursors for metal sulfide preparations, especially as their lower alkyl derivatives are generally crystalline solids but are significantly volatile. Wold and co-workers⁵¹ have studied the decomposition products of [Zn(S₂CNEt₂)₂] using GC-MS and reported the deposition pathway involves clean elimination of ZnS from the precursor (eqn (1) and (2)). However, the proposed decomposition route is somewhat different to the stepwise fragmentation observed in the EI-MS of the compound (eqn (3)). This

difference can be attributed to inherent differences between the two techniques.



In contrast, the analogous diethyldiselenocarbamates have been shown to be poor sources for the deposition of ZnSe or CdSe films. Under similar reaction conditions (10^{−3}–10^{−4} Torr, 370–420 °C) the diethyldiselenocarbamate precursors give films of the metal selenide heavily contaminated with selenium.⁵² However, the mixed-alkyl diethyldiselenocarbamate complexes [MeM(Se₂CNEt₂)] (M = Cd, Zn) proved to be suitable for MSe (M = Cd, Zn) thin films.^{53,54} Later, ZnSe films were deposited from [Zn(Se₂CNMe(C₆H₁₃))₂] which has two different alkyl substituents at the nitrogen. This complex is monomeric in the solid phase⁵⁵ in contrast to the analogous diethyldiselenocarbamates and the mixed alkyl-diethyldiselenocarbamates complexes, which are dimers. The decomposition of *N,N*-dialkyldithiocarbamate complexes is believed to occur through a free radical decomposition route, which is consistent with the formation of disulfide products from the thermal decomposition of these complexes.⁵⁶ It has also been noted that *N,N*-dialkyldithiocarbamate complexes are more stable than their corresponding *N*-alkyldithiocarbamate complexes due to the lack of acidic hydrogen atoms at the nitrogen.⁵⁷

An interesting application of the comproportionation reaction is the preparation of mixed species such as methylcadmium– or methylzinc–diethyldiselenocarbamates that are useful for deposition of thin films of ternary solid solutions of Cd_{0.5}Zn_{0.5}Se. Polycrystalline Cd_{0.5}Zn_{0.5}Se layers, for which the band gap was estimated as 2.1 eV, were deposited on glass substrates by low pressure MOCVD. The mixed aggregate showed similar dimeric molecular units [RMSe₂CNEt₂]₂ to other alkylmetal dithio- or diseleno-carbamates. In the solid state structure, cadmium and zinc atoms were modeled as randomly occupying the metal sites.⁵⁴

Metal complexes of the imino-bis(diphenylphosphine chalcogenide) ligand [NH(PPh₂Se)₂] are suitable as single-source precursors for MSe (M = Cd, Zn) thin films.⁵⁸ In CVD applications complexes of the isopropyl derivatives are better in view of their higher volatility as compared to those of the phenyl-substituted derivatives.⁵⁹ Recently Chivers and co-workers have reported the ditelluro-analogues (tmeda)Na[N(TePR₂)₂] (R = Ph, ^{*i*}Pr)^{60,61} of which the isopropyl substituted ligand has been used in metathetical reactions with metal halides to generate homoleptic complexes of the type M[(TeP^{*i*}Pr)₂N]₂ (M = Zn, Cd, Hg). The usefulness of such compounds has been demonstrated in aerosol-assisted (AA)CVD experiments⁶² and has been reviewed.⁶³

3 Chemical bath deposition (CBD)

There is considerable interest at present in the soft processing of materials. Chemical bath deposition (CBD), also known as chemical solution deposition, is a simple, convenient and

inexpensive method for depositing thin films.⁶⁴ The CBD process uses a controlled chemical reaction to effect the deposition of a thin film by precipitation. Films may be deposited at low temperatures on a variety of substrates. The thickness of the deposited layers may be readily controlled by variation of the deposition time. The process should be easily adaptable to large area processing with low fabrication cost.

3.1 Zinc oxide thin films

There is a considerable and dispersed literature describing zinc oxide (ZnO). The thermodynamic stable crystallographic phase of ZnO is the hexagonal wurtzite structure.⁶⁵ Control of the size, shape and orientation of ZnO crystallites on the substrates is often a prerequisite for creation of high surface area materials for use in many types of devices including hybrid photovoltaics and optoelectronic devices.

The formation of high-aspect ratio ZnO crystallites has attracted interest.⁶⁶ It has been suggested that “Zn(OH)₂” is a prerequisite for the growth of needle-like ZnO crystallites.⁶⁷ Hexamethylenetetramine (HMT) is widely used in the growth of acicular ZnO thin films. Fujita *et al.*,⁶⁸ have reported controlled synthesis of ZnO crystallites using HMT. The precipitates derived from zinc nitrate were globular or rod-shaped whereas those from zinc chloride were both globular and acicular. The rod-like ZnO arrays have been deposited on fluorine doped tin oxide (TO(F)) substrates using zinc nitrate–HMT solutions in closed vessels.⁶⁹ ZnO nanostructured layers comprising layers nanorods, tripods or hexagonal platelets have been also grown at temperatures around 500 °C by a simple spray pyrolysis method.⁷⁰ Experimental results obtained indicate that shape and size-controlled synthesis of ZnO nanostructures can be achieved by adjusting the concentration of precursors, deposition temperature, solvent and substrate type.

We have reported the growth of perpendicularly orientated ZnO rods on thin ZnO templates, from aqueous baths containing zinc acetate and HMT.⁷¹ The use of a ZnO template allows tailoring of the surface density of the rods. It has also been shown that the quality of ZnO rods being produced strongly depends on the ligand as well as counter ion in the baths. Moreover, white-light luminescence and room-temperature lasing throughout the visible has been demonstrated for the first time for ZnO nanocolumns grown on Au-coated tin-oxide glass.⁷² The directionality of the emission, lasing threshold and observed mode were all consistent with Fabry–Pérot lasing cavities. We have hence demonstrated the potential of ZnO nanocolumns, grown by solution deposition, as a miniature broadband visible-light source.

More recently, we have reported a general solution-based approach for growing orientated ZnO nanostructured films,⁶⁴ and have shown that the morphology of the particles is strongly dependent on the nature of base *e.g.* ethylenediamine (en) usually gives rise to starlike crystals, triethanolamine (TEA) produces nodules and HMT usually produces rods (Fig. 2). Similarly, changing the counter-ion of the zinc salt also has been shown to produce different crystallite morphologies on TO(F) glass substrates. No films were successfully

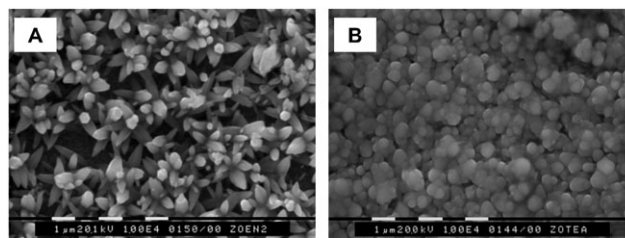


Fig. 2 SEM images of ZnO films from baths (70 °C, pH 11): (A) starlike crystallites from en–zinc acetate; [Zn] = 0.018 mol dm^{−3}, [en] = 0.042 mol dm^{−3}; (B) dense nodular grains from TEA–zinc nitrate baths; [Zn] = 0.018 mol dm^{−3}, [TEA] = 0.072 mol dm^{−3}.⁶⁴

grown from zinc sulfate containing baths. Relatively poor dense films having acicular crystallites were deposited from zinc chloride, perchlorate and nitrate on TO(F) glass. Dense films were deposited from zinc acetate containing baths but the rod-like crystallites were not well orientated. From the results, it became clear that counter-ions have a noticeable effect on the morphology of the films.

The dimensions of crystallites varied significantly for each of the different systems used. In agreement with earlier observations, no films were deposited using zinc sulfate. It is expected that the presence of sulfate anions hinders the heterogeneous nucleation/growth processes on ZnO templates which would otherwise precede the homogenous process. Films deposited from baths containing acetate, formate and chloride were more homogenous than those containing perchlorate and nitrate.

Deposition experiments were performed using HMT–zinc acetate baths with different substrates, *viz.* gold-coated TO(F) glass, ZnO template layers on TO(F) glass and TO(F) glass (Fig. 3). There was a noticeable difference between the width of the rods but their lengths were similar. Furthermore, films deposited on Au-coated TO(F) substrates and ZnO template layers were well-aligned.

The influence of bath pH on as-deposited films of ZnO, grown on ZnO template layers, using zinc acetate–HMT was investigated. The homogeneous precipitation occurred more rapidly in zinc acetate–HMT systems where no pH adjustment was made, compared to those where the pH was lowered. The films deposited from baths for which no pH adjustment was made, comprised of different grain sizes with poorly developed crystal faces. In subsequent experiments, baths were adjusted to pH = 5. For the latter conditions, films were comprised of rods with well-defined faces and in addition, the individual particles had a smaller diameter than those obtained from the former experiments.

Previously, it has been determined that bath temperature and growth time have a profound effect on crystal morphology. For ZnO grown under hydrothermal conditions, an increase in bath temperature for solutions containing ZnCl₂ and HMT resulted in a change in morphology from rods to needles.⁷³ The length and final shape of rods were dependent on the growth time. Zhang *et al.* have established that ageing time also has a significant influence on final morphology, *i.e.*, ZnO habit changes from flaky aggregates to a flower-like morphology with increasing growth time.⁷⁴ The growth of

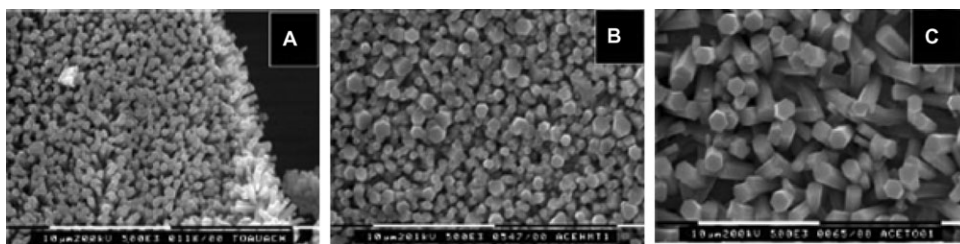


Fig. 3 SEM images of ZnO films from HMT baths ($0.025 \text{ mol dm}^{-3} \text{ Zn}(\text{CH}_3\text{COO})_2$ and $0.025 \text{ mol dm}^{-3}$ HMT, pH 5, 90°C , 1 h) on (A) Au-coated TO(F) glass; (b) ZnO template layers on TO(F) glass and (C) TO(F) glass.⁶⁴

ZnO rod array films (using zinc acetate) on ZnO template layers as a function of deposition time was investigated.⁶⁴ Films removed from baths after different time intervals indicated that crystallites had an average diameter of $\sim 300 \text{ nm}$ after 2 min and $\sim 1 \mu\text{m}$ after 1 h. Table 2 lists the average rod dimensions for the different deposition times. It was only possible to determine the average rod length for those grown for greater than 10 min. For shorter growth times, it proved difficult to distinguish the template layer from the ZnO rod growth.

The use of ZnO nanorod arrays in hybrid polymer/metal oxide solar cells has been studied.⁷⁵ Different solution chemical routes were investigated for the synthesis of the inorganic device components, *i.e.* the ZnO columnar structures and the “backing” layers, which act as a seed-growth layer for the ZnO rods. It has been observed that the growth of the ZnO nanorod arrays is dependent on the morphological and structural characteristics of the seed layer, but also that the seed layer itself is affected by the synthetic conditions of rod growth. Different polymers (high hole-mobility MEH-PPV based polymer and P3HT) were compared in these structures and power conversion efficiencies of 0.15 and 0.20% were achieved under 1 Sun illumination, respectively.

3.2 Zinc sulfide thin films

CBD is a useful method for the deposition of zinc sulfide (ZnS) thin films. It is also a method free of many inherent problems associated with high-temperature techniques such as MOCVD, especially evaporation of ZnS leading to polysulfides and the limited choice of substrates. The CBD-ZnS films have been investigated as a buffer layer alternative to CdS in polycrystalline thin film $\text{Cu}(\text{In}_{1-x}\text{Ga}_x)\text{Se}_2$ (CIGS) solar cells.⁷⁶ Cells with efficiency up to 18.1% based on CBD-ZnS/CIGS heterostructures have been fabricated.

The deposition of ZnS by CBD is more difficult than CdS, due to a much wider range of conditions within which the

concurrent deposition of ZnS and/or ZnO may occur.⁷⁷ Many of the films reported as ZnS are probably heavily contaminated with ZnO or $\text{Zn}(\text{OH})_2$. Mokili *et al.*⁷⁸ have showed that CBD deposits contained significant amounts of oxygen. EXAFS studies have confirmed the presence of oxygen in the form of hydroxide and a high oxygen to sulfur ratio. Some films were even reported as $\text{Zn}(\text{OH})_2$.

The formation of good quality ZnS films appears to be favored in the presence of ammonia and hydrazine. The dominant effect of the second ligand may be to enhance the decomposition of thiourea by increasing the rate of sulfidization of the growing film. In this reaction system, ammonia forms $[\text{Zn}(\text{NH}_3)_4]^{2+}$, controlling the concentration of free Zn^{2+} and also keeping the pH within a suitable range for the reaction involving thiourea.^{79–83} Lincot and Ortega-Borges⁸⁴ have reported that the use of ammonia and thiourea without hydrazine results in films which are not homogeneous or adherent. Similarly, Dona and Herrero⁸⁵ have suggested that the addition of hydrazine improved the homogeneity and growth rate of ZnS films. The authors have suggested that the rate-determining step for the heterogeneous process may involve the dissociation of a $\text{Zn}^{2+}\text{--L}$ bond. This seems unlikely as zinc is a classic example of a labile metal-ion. Another suggestion made was that the hydrazine complex ions have a lower coordination number. Hydrazine could potentially act as a bridging ligand and perhaps facilitate surface binding.

Our earlier calculations support a number of remarks relating to the conditions most suited to the deposition of ZnS⁷⁹ (i) equivalent levels of supersaturation for the sulfide are typically found at pH values *ca.* 2.5 lower for ZnS than for CdS, (ii) if reactions are carried out in a high pH regime, more sulfiding agent will be required for the zinc system and (iii) at lower pH, the rate of hydrolysis of the sulfide source is likely to be reduced. Even if a lower pH is used, more sulfide source might be required. Bath conditions similar to those described herein have previously been reported,⁸⁶ the solution contained zinc ions, urea and thioacetamide at modestly acidic pH values. The films deposited using such a method were found to exhibit band gaps close to that expected for ZnS. Ternary materials such as $\text{Cd}_{1-x}\text{Zn}_x\text{S}$ can also be successfully deposited in moderately acidic baths.⁸⁷

Adherent and uniform ZnS films had been deposited reproducibly by CBD, under acidic conditions from solutions containing ZnCl_2 , urea and thioacetamide.⁷⁷ The quartz crystal microbalance studies suggested that film growth occurred after a short induction period, *via* an initial rapid phase

Table 2 Rod dimensions of ZnO films deposited on microcrystalline ZnO templates for different deposition times⁶⁴

Time/min	Average rod width/ μm	Average rod length/ μm
2	0.3	nd
5	0.5	nd
10	0.5	nd
20	0.75	~ 1.25
30	0.75	~ 1.5
60	~ 1	~ 2

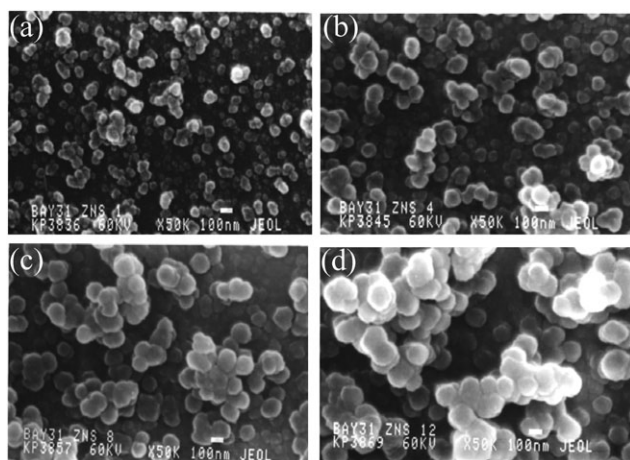


Fig. 4 SEM images of CBD-deposited ZnS films grown over (a) 900; (b) 3600; (c) 7200 and (d) 10800 s.⁷⁷

(deposition rate of 91 nm h^{-1}), followed by a slower process (growth rate of 52 nm h^{-1}). The samples removed at regular intervals, suggested that as the reaction proceeds, uniform film growth is associated with increasing particle size, rather than deposition of new primary particles (Fig. 4). The numerical values for the mean radii of 23.70, 37.42, 51.01 and 71.13 nm were obtained, for deposition over 900, 3600, 7200 and 10800 s, respectively. Grain size distributions have been investigated using computational image analysis, and an average grain growth rate of 33.7 nm h^{-1} has been calculated.

4 Liquid–liquid Interface

The potential for the use of the interface between two liquids to synthesize materials is interesting because it provides a direct route for the growth of nanocrystals anchored to the surface in the form of a film.^{88–90} Films can be deposited at low temperatures and subsequently transferred to a variety of substrates. The thickness and other characteristics of the deposited layers may be controlled by variation of the deposited parameters such as deposition time. The process is potentially easily adaptable to large-area processing with low fabrication cost.⁹¹

Rao *et al.* have reported highly crystalline ZnO films by the reaction of zinc cupferronate in toluene and an aqueous solution of sodium hydroxide at 25°C .⁸⁹ The films were composed of hexagonal ZnO with a preferred orientation along the (100) plane. Sonification of the films yielded both 1D and 2D structures with different dimensions. Same authors have deposited single-crystalline ZnS films using zinc cupferronate in the presence of Na_2S .⁹² More recently, we improved ZnS deposits at the interface by using zinc diethyldithiocarbamate as a zinc source and Na_2S as a sulfide source at the water/toluene interface.⁹³ The deposited films consisted of large micron-size grains with hexagonal zinc-blende structure. Accordingly, the optical band gap of the films (3.5 eV) was close to the bulk value (3.6 eV). The SEM images of ZnS thin films on quartz substrates revealed that the films consist of flakes with dimensions of $\sim 500 \text{ nm}$ (Fig. 5).

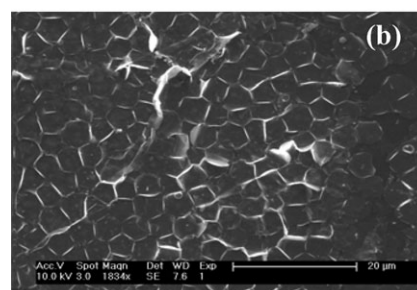
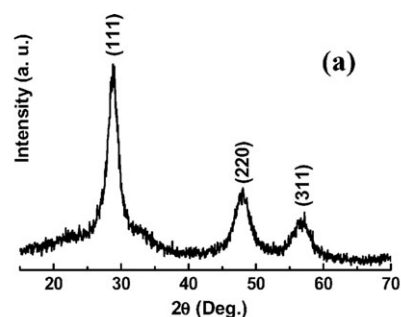


Fig. 5 (a) XRD pattern and (b) SEM image of cubic ZnS thin film deposited at a liquid–liquid interface.⁹³

5 Nanodimensional materials

There has been substantial interest in the preparation and characterisation of materials consisting of particles with dimensions in the order of $2\text{--}100 \text{ nm}$, so-called “nanocrystalline materials”. The possibility of engineering band gap and influencing physical, chemical and electrical properties by varying the dimensions of the system has provided a strong impetus to study nanocrystals and other nanodimensional materials. Two fundamental factors, both relating to the size of the individual nanocrystal, are responsible for unique properties seen in semiconductor nanoparticles.⁹⁴ The first is the large surface-to-volume ratio; as a particle becomes smaller the ratio of the number of surface atoms to those in the interior increases, with greater than a third of all atoms residing on the surface in very small particles. This leads to surface properties playing an important role in the overall properties of the material. The second factor is the actual size of the particle; with semiconductor nanoparticles there is a change in the electronic properties of the material, the band gap gradually becoming larger because of quantum confinement effects as the size of the particles decreases. This effect is a consequence of the confinement of a “particle in a box” giving rise to discrete energy levels similar to those in atoms and molecules, rather than a continuous band as in the corresponding bulk semiconductor material.

5.1 ZnO nanocrystals

Nanocrystals of ZnO with various diameters have been obtained using different chemical routes including arrested precipitation and sol–gel techniques based on the hydrolysis of zinc salts.^{95–98} Studies on ZnO nanocrystals prepared by the above methods have yielded useful results. For example, the variation of band gap in ZnO nanocrystals is strongly size-dependent below a diameter of $\sim 7.0 \text{ nm}$.^{99,100} However, the

ionic species used to influence growth often get adsorbed on the surface of the nanocrystals along with a hydroxylated layer, preventing effective capping and introducing surface states and other defects in the nanocrystals.^{101,102} Further, these sols possess limited stability. Non-hydrolytic routes employing metal-organic precursors have, therefore, become important. Shim and Guyot-Sionnest¹⁰³ have synthesized ZnO by thermolysis of Et₂Zn in trioctylphosphine oxide (TOPO) in the presence of oxygen. The nanocrystals obtained under these conditions have high defect densities. In fact, the fluorescence spectra of these nanocrystals only consist of defect emission bands. It is generally believed that syntheses carried out using single-source precursors that contain preformed Zn–O bonds could yield ZnO nanocrystals with low defect densities. Thus, [Zn(CH₃CH₂OO)₂], [EtZnOⁱPr] and [MeZnOSiMe₃]₄ have been decomposed under various conditions to yield ZnO nanocrystals.^{104–106} However, defect related emission still dominates the emission from such particles. There has been some limited success recently in synthesizing ZnO nanocrystals with low defects.^{107–109} Despite these advances, the synthesis of ZnO nanocrystals with low defect densities still possess significant challenges.

We have reported the growth of ZnO nanocrystals by thermal decomposition of single-source precursors: zinc cupferronate [Zn(C₆H₅N₂O₂)₂] and zinc ketoacidoximate: [Zn(C₈H₁₆N₂O₈)].¹¹⁰ Octylamine-coated ZnO nanocrystals with diameters in the range of 7.0–14.0 nm were obtained by decomposition of zinc cupferronate. Smaller nanocrystals, with diameters in the range of 3.9–6.5 nm, were obtained by decomposition of zinc oximate. ZnO nanocrystals grown by this method possess low defect densities and exhibit band edge luminescence. Quantum confinement effects as indicated by the blue shift of absorption onset are apparent in all nanocrystals and are particularly strong in those with diameters less than 7 nm.

There has been a lot of interest in doping ZnO with 3d transition metal ions because of potential application in spin based electronic (spintronics) since prediction made by Dietl *et al.* that Mn-doped ZnO would be ferromagnetic at room temperature.¹¹¹ Studies on bulk and nanocrystalline ZnO doped with 3d transition metal ions are primarily concerned with the magnetic properties.^{109–115} A few studies have suggested that ZnO doped with transition metal ions could possess interesting optical properties.^{116–120}

Previous attempts at doping nanocrystals have been fraught with problems because the synthetic schemes used to dope frequently yield inhomogeneously doped materials. The frequent failure of doping schemes was, until recently, attributed to the expulsion of dopant ions to the surface of nanocrystals by the intrinsic process of self-annealing. Efros and co-workers have suggested that doping is directly related to the stability of the ions to adsorb to the exposed surfaces of the nanocrystals rather than self-annealing.¹²¹ It appears, therefore, that successful doping of nanocrystals can be achieved by involving nanocrystals of the right size and morphology and choosing surfactants that do not bind too strongly to the dopant ions.

We have reported the changes in the optical properties of ZnO nanocrystals brought about by successful doping with Mg, Cd, Fe and Mn ions using a family of metal cup-

ferrates.¹²² We performed such doping for ZnO nanocrystals with diameters in a range unaffected by quantum effects (> 7.0 nm).^{99,100} XRD patterns of pure and doped nanocrystals reveal the presence of a single hexagonal phase with the zincite structure, indicating that phase-pure doped nanocrystals were obtained. Magnesium ions introduced as dopants at levels below 10% shifted the diffraction peaks to higher angles, suggesting that the unit cell contracts to accommodate the ions. A change is expected if Mg ions replace Zn ions in the lattice, as the Mg ions have smaller ionic radii. Higher levels of Mg led to a broadening of the peaks with shifts indicating an expansion of the unit cell, possibly due to the Mg ions preferring to occupy interstitial sites. Doping with Cd ions also led to expansion of the lattice depending on the doping level. Doping with Mn ions produced no appreciable shift in the lattice parameters since both ions possess similar radii. Shifts indicating a small increase in the unit cell dimensions were as seen in the case of Fe. The presence of small amounts of Mn and Mg ions (up to ~2%) influences the growth process, resulting in elongated nanocrystals. Simply increasing the concentrations of the dopant ions yields spherical nanocrystals.

The shifts in the optical band gap in ZnO caused by doping with Mg, Cd and Mn ions are summarized in Fig. 6.¹²² The band gap of the ZnO nanocrystals could be tuned in the range of 2.92–3.77 eV by the use of Mg and Cd ions as dopants. The energy difference of 0.85 eV between the highest and lowest band gaps in doped nanocrystals is substantially higher than that typically achieved in ZnO nanocrystals. Mg doping shifted the absorption onset to blue, indicating an increase in the band gap. Doping with Cd, on the other hand, produced a red shift indicative of a decrease in the band gap. The optical band gap fell nearly linearly from 3.30 to 2.92 eV with the increase of Cd doping levels from 0 to 10%. The systematic and linear shifts with doping levels suggested that the introduction of dopant ions, rather than size effects, brings about these changes. The introduction of transition metal ions quenches the luminescence of the nanocrystals. We believe that successful doping in this case is due to the choice of precursors with similar volatility and is also due to the larger size of nanocrystals employed in this study.

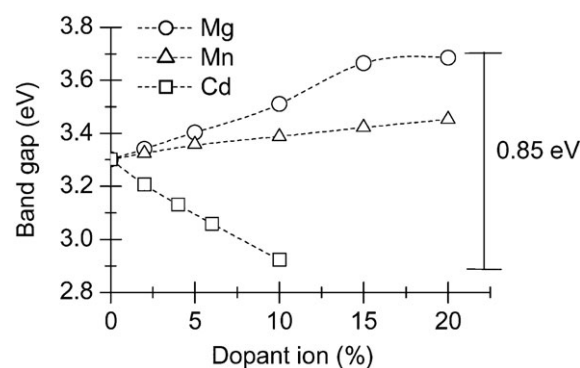


Fig. 6 Plot showing the changes in the optical band gap in ZnO nanocrystals that accompanies doping with different ions. The ions as well as the doping levels are indicated in the plot.¹²²

5.2 Molecular precursor based approach for zinc chalcogenide nanoparticles

Many synthetic methods for the preparation of nanodispersed materials have been reported, with several routes applying conventional colloidal chemistry.^{123–130} Controlled precipitation reactions yield dilute suspensions of quasi-monodispersed compounds. This synthetic method sometimes involves the use of seeds of very small particles for the subsequent growth of larger ones.^{131,132} A powerful method for the preparation of semiconductor nanocrystallites has been described by Bawendi and co-workers.¹³³ Solutions of $(\text{CH}_3)_2\text{Cd}$ and trioctylphosphine selenide (TOPSe) are injected into hot trioctylphosphine oxide (TOPO). This produced TOPO capped nanocrystallites of CdSe. The size distribution of the particles is controlled by the temperature at which synthesis is undertaken with larger particles being obtained at higher temperatures. Hines and Guyot-Sionnest¹³⁴ used a similar methodology involving dimethylzinc and TOPSe as precursors. However, the use of TOPO/TOP as capping agents failed and a mixture of hexadecylamine (HDA) and TOPO was used instead. However, the reaction conditions are harsh and involve hazardous, toxic, and in the case of metal alkyls, pyrophoric materials. These precursors are injected into hot solutions (up to 350 °C), which may be undesirable for commercial exploitation since dimethylcadmium and dimethylzinc are volatile, toxic, pyrophoric compounds with relatively low boiling points.

One alternative to metal alkyls for the synthesis of chalcogenide nanoparticles involves the use of single-source precursors. Some of the single-source precursors used for nanocrystals are shown in Fig. 7. Our research has focused on a rational approach using single-source precursors to develop methods of nanoparticle synthesis. There are a number of potential advantages of using single-source precursors over other existing methods including: improved air/moisture stability, limited pre-reaction and control of stoichiometry. We have extensively investigated the synthesis of ME ($\text{M} =$

Cd, Zn; $\text{E} = \text{S}, \text{Se}$) quantum dots and related core-shell composites from bis(alkyldithio/diselenocarbamates) of Zn and Cd.^{135,136} The synthesis involves the dissolution of the precursor in TOP followed by decomposition in a suitable high-boiling coordinating solvent (TOPO or 4-ethylpyridine), usually at 200 °C. The size of the as-synthesised nanoparticles depends on the reaction time and temperature, precursor/capping agent ratio, and alkyl groups. For example, in the case of zinc, symmetrical or unsymmetrical alkyl groups lead to good quality ZnS ¹³⁷ and ZnSe ¹³⁸ quantum dots. The synthesis of the precursor is a simple, two-step procedure that requires first the preparation of the (dialkyldithio-/diselenocarbamato)dialkylammonium salt by treating CS_2 or CSe_2 with an excess of a secondary amine at 0 °C, followed by reaction with an aqueous solution of metal salts. The zinc chalcogenolato complexes $(N,N'\text{-TMEDA})\text{Zn}(\text{EPh}_2)$ ($\text{E} = \text{Se}, \text{Te}$) have been employed to yield monodispersed zinc chalcogenide nanoparticles.¹³⁹ The growth of nanoparticles follows a simple ligand elimination reaction and by varying the growth temperature it is possible to control their size.

Preliminary studies have also been carried using the zinc thiocarboxylate compounds; $[\text{Zn}(\text{SOCR})_2(\text{Lut})_2]$ [$\text{R} = \text{CH}_3, \text{C}(\text{CH}_3)_3$; Lut = 3,5-dimethylpyridine (lutidine)].¹⁴⁰ The compounds are prepared from the reactions of Et_2Zn with thioacetic and thiopivalic acids and results in nearly quantitative yields of pure, highly crystalline products, since the only byproduct is ethane which can be removed easily. The $[\text{Zn}(\text{SOCCH}_3)_2(\text{Lut})_2]$ was thermally decomposed in toluene to yield amorphous ZnS with an average size of 5.0 nm. The compound was expected to undergo thiocarboxylic anhydride elimination to give stoichiometric ZnS and remove the organic supporting ligands cleanly. Under identical conditions, $[\text{Zn}(\text{SOC}(\text{CH}_3)_3)_2(\text{Lut})_2]$ exhibited very little decomposition in toluene and pyridine. Extensive heating and stirring in toluene for 36 h at 120 °C did not result in complete decomposition.

In order to obtain a narrow size distribution without any further post preparative separation treatment such as selective precipitation, single-source molecular inorganic clusters have been employed. The clusters used have discrete units within core structures related to that of bulk semiconductor materials $[\text{M}_{10}\text{Se}_4(\text{SPh})_{16}][\text{X}]_4$ ($\text{M} = \text{Cd}, \text{Zn}$; $\text{X}^+ = \text{Li}^+, \text{Me}_3\text{NH}^+$).¹⁴¹ CdSe particles were grown using $\text{X} = \text{Li}$ and ZnSe particles grown using $\text{X} = \text{Me}_3\text{NH}$. Because of the complete separation of nucleation and growth this method showed a high degree of control over particle size. Once the desired particle size is obtained, as established from UV spectra of aliquots of the reaction solution, the temperature is reduced by ca. 30–40 °C and the mixture left to “size focus” for 12 h. The average particles distribution is thereby narrowed due to Ostwald ripening, in a process where small crystallites are less thermodynamically stable than larger ones and thus dissolve more readily into their respective ions. This method can produce batches of particles with narrow size distributions in the 2.5–9.0 nm range for CdSe and 3.0–5.0 nm range for ZnSe. By post-treating CdSe particles with solutions of Me_2Zn and $(\text{Me}_3\text{Si})_2\text{S}$, core-shell particles of CdSe/ZnS can be formed with quantum yields enhanced by a factor of >2 (6–20%).¹⁴¹

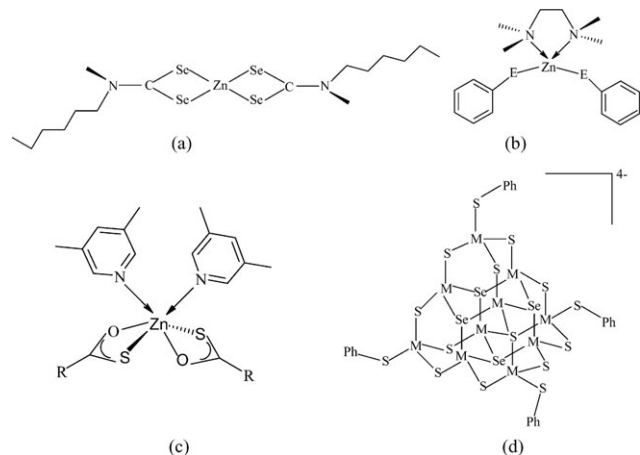


Fig. 7 Structures of single-source precursors used for zinc chalcogenide nanocrystals (a) $[\text{Zn}(\text{Se}_2\text{CNMe}(\text{C}_6\text{H}_{13})_2)_2\text{N}]$; (b) $(N,N'\text{-TMEDA})\text{Zn}(\text{EPh}_2)$ ($\text{E} = \text{Se}, \text{Te}$); (c) $[\text{Zn}(\text{SOCR})_2(\text{Lut})_2]$ [$\text{R} = \text{CH}_3, \text{C}(\text{CH}_3)_3$; Lut = 3,5-dimethylpyridine (lutidine)]; (d) $[\text{M}_{10}\text{Se}_4(\text{SPh})_{16}][\text{X}]_4$ ($\text{M} = \text{Cd}, \text{Zn}$; $\text{X}^+ = \text{Li}^+, \text{Me}_3\text{NH}^+$).

Precursors based on zinc trimethylsilylchalcogenolate complexes (N,N' -TMEDA) $Zn(E\text{SiMe}_3)_2$ ($E = \text{S}, \text{Se}$) and $(3,5\text{-Me}_2\text{-C}_6\text{H}_3\text{N})_2Zn(E\text{SiMe}_3)_2$ have been investigated for zinc chalcogenide nanoparticle syntheses.¹⁴² In solution, the complexes decompose cleanly and under mild conditions by the generation and elimination of $E(\text{SiMe}_3)_2$ and the partial loss of amine/imine ligands to produce ZnS or $ZnSe$ nanoparticles whose surfaces are protected by either N,N' -TMEDA or lutidine. Dynamic light scattering experiments indicate that the particles have sizes in the 2–3 nm range. Similar chemistry in the solid state leads to the formation of size-restricted ZnS and $ZnSe$ materials, however only with N,N' -TMEDA ligated complexes generate particles that are within the quantum confinement regime.

Nanocrystals of ZnS (rods or dots) have been prepared by the thermolysis of zinc ethylxanthate [$Zn(\text{C}_2\text{H}_5\text{OCS}_2)_2$] in octylamine (OA) or TOP.¹⁴³ Shape- and phase-controlled synthesis of the ZnS nanocrystals was realized by the selection of different ligands. In the HDA + OA system, wurtzite ZnS nanorods are obtained in the temperature range of 150–250 °C. In HDA + TOP system, a shape change from rod-like to spherical particles and a phase transition from wurtzite to sphalerite occurred with the increase of TOP content in the solution. The absorption edge of the wurtzite ZnS nanorods shifted blue as compared to that of the sphalerite nanodots. In addition, there are two absorption peaks for the ZnS nanorods formed at 150 °C with a high aspect ratio and diameters in the strong quantum confinement range. For the PL spectra of the ZnS nanocrystals, there is a relatively strong excitonic emission peak for the ZnS nanodots formed in the HDA + TOP solution and a relatively strong interstitial atom emission for the ZnS nanorods.

More recently, our investigations have been focused on the synthesis of selenophosphinate ligands which might serve as useful precursors for metal selenides. Initially, we reported a facile route for the preparation of $(R_2PSe)_2Se$ ($R = \text{Ph}, ^i\text{Pr}$) in *ca.* 45% yield.¹⁴⁴ Further investigations on diselenophosphinate ligands led to the isolation of the $(R_2PSe_2)^-$ anion crystallised as an alkylammonium salt in the form of $(\text{HNET}_3)(R_2PSe_2)$ ($R = ^i\text{Pr}, ^t\text{Bu}, \text{Ph}$).¹⁴⁵ The zinc complex $[Zn(^i\text{Pr}_2PSe_2)_2]$ was thermolysed in HDA, to yield hexagonal $ZnSe$ nanorods. The HR-TEM image of individual nanorods revealed regularly spaced lattice fringes with a separation of 0.35 nm, consistent with the (100) lattice planes (Fig. 8).

Little attention has been directed at the synthesis of ternary II–II'–VI nanoparticles using single-source precursors. The band gap energy can be tuned by controlling both the size of the nanoparticles and the metal-ion stoichiometry (*i.e.* the ratio of M/M'). The ternary cluster compounds are ideal candidates for the synthesis of ternary nanoparticles in which the Zn/Cd ratio of the final products can be modulated by the adjustable stoichiometry. The ternary molecular nanoclusters $[Zn_xCd_{10-x}E_4(\text{EPh})_{12}(\text{P}^i\text{Pr}_3)_4]$ ($x = 1.8, 2.6$; $E = \text{Se}, \text{Te}$) have been employed as single-source precursors for the synthesis of high-quality hexagonal $Zn_xCd_{1-x}E$ nanocrystals.¹⁴⁶ The thermolysis of the cluster molecules in HDA provided an efficient system in which the inherent metal-ion stoichiometry of the clusters was retained in the nanocrystalline products, whilst also affording control of particle size within the 2–5 nm range.

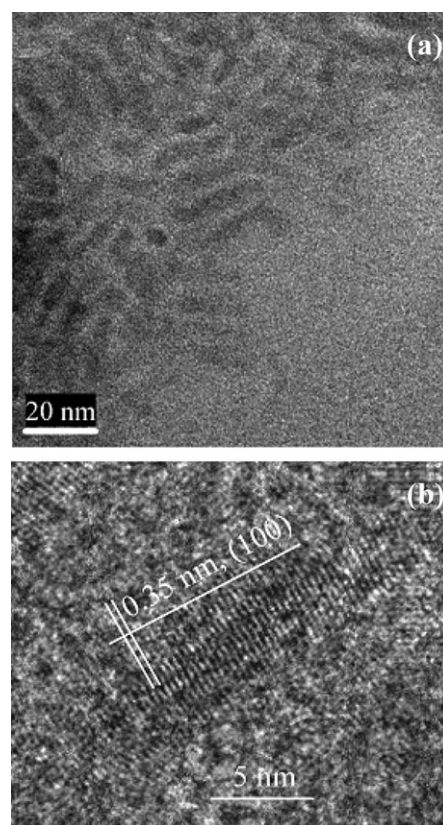


Fig. 8 (a) TEM and (b) HR-TEM of $ZnSe$ nanorods.¹⁴⁵

In all cases, the nanoparticles were monodispersed and luminescence spectra exhibited emissions energies close to the absorption edge.

6 Conclusions

This article provides an overview of a variety of methods and starting materials available for the fabrication of zinc oxide or chalcogenides. Current research involves on developing next-generation precursors to overcome problems such as non-stoichiometry and the incorporation of impurities within the generated materials.

It is believed that the nanomaterials will find important applications in various areas including information technologies, biotechnologies, and energy/environmental technologies. In particular, different kinds of nanocrystals have been extensively used, in biomedical applications and biosensors.¹⁴⁷ For example, magnetic nanocrystals have been applied to contrast enhancement agents for magnetic resonance imaging, magnetic carriers for drug-delivery systems and biosensors.¹⁴⁸

Intensive research has been conducted on the assembly of monodisperse nanocrystals to form two- and three- dimensional superlattice structures. These organized nanoparticles exhibit novel physical properties that derive from their collective interaction, and which are essential for magnetic storage media and electronic devices.¹⁴⁹

The use of ZnO nanocrystals in hybrid polymer, low-cost, environmentally friendly solar cells is particularly attractive. A judicious choice of different sizes and shapes may further

improve charge transport and energy conversion in such solar cells.

Acknowledgements

The authors thank RCUK and the EPSRC for funding and various O'Brien group members past and present who have contributed to the work described herein.

References

- O. Madelung, *Semiconductors—Basic Data*, Springer, Berlin, 2nd edn, 1996, pp. 182–184 and 190–192; ISBN: 3-540-60883-4.
- R. A. Sorel, *J. Vac. Sci. Technol., A*, 1996, **14**, 913.
- Y. C. Zhu, Y. Bando, D. F. Xue and D. Golberg, *Adv. Mater.*, 2004, **16**, 831.
- M. Ihara, T. Igarashi, T. Kusunoki and K. Ohno, *J. Electrochem. Soc.*, 2002, **149**, H72.
- P. T. Tran, E. R. Goldman, G. P. Anderson, J. M. Mauro and H. Mattoussi, *Phys. Status Solidi G*, 2002, **229**, 427.
- E. R. Goldman, E. D. Balighian, H. Mattoussi, M. K. Kuno, J. M. Mauro, P. T. Tran and G. P. Anderson, *J. Am. Chem. Soc.*, 2002, **124**, 6378.
- (a) D. Moore and Z. L. Wang, *J. Mater. Chem.*, 2006, **16**, 3898; (b) X. Fang and L. Zhang, *J. Mater. Sci. Technol.*, 2006, **22**, 721.
- (a) D. More, Y. Ding and Z. L. Wang, *Angew. Chem., Int. Ed.*, 2006, **45**, 5150; (b) X.-S. Fang, C.-H. Ye, L.-D. Zhang, Y.-H. Wang and Y.-C. Wu, *Adv. Funct. Mater.*, 2005, **15**, 63; (c) K. Wright and J. D. Gale, *Phys. Rev. B*, 2004, **70**, 035211; (d) G. Moh, *Chem. Erde*, 1975, **1**, 134; (e) P. Gardner and P. Pang, *J. Chem. Soc., Faraday Trans. 1*, 1988, **84**, 1879.
- T. Matsuoaka, *Adv. Mater.*, 1996, **8**, 469.
- R. Passler, E. Griebel, H. Ripel, G. Lautner, S. Bauer, H. Preis, W. Gebhardt, B. Buda, D. J. As, D. Schikora, K. Lischka, K. Papagelis and S. Ves, *J. Appl. Phys.*, 1999, **86**, 4403.
- J. Wang, D. C. Hutchings, A. Miller, E. W. Vanstryland, K. R. Welford, I. T. Muirhead and K. L. Lewis, *J. Appl. Phys.*, 1993, **73**, 4746.
- L. Li, Y. Yang, X. Huang, G. Li and L. Zhang, *J. Phys. Chem. B*, 2005, **109**, 12394.
- D. W. Kisker, *J. Cryst. Growth*, 1989, **98**, 127.
- W. S. Kuhn, B. Qu'Hen, O. Gorochov, R. Triboulet and W. Gebhardt, *Prog. Cryst. Growth Charact. Mater.*, 1995, **31**, 45.
- K. J. Wilkerson, M. J. Kappers and R. F. Hicks, *J. Phys. Chem. A*, 1997, **13**, 2451.
- M. Huang, S. Mao, H. Feick, H. Yan, Y. Wu, H. Kind, E. Weber, R. Russo and P. Yang, *Science*, 2001, **292**, 1897.
- W. L. Bragg and J. A. Derbyshire, *Trans. Faraday Soc.*, 1932, **28**, 522.
- Structure Reports*, ed. W. B. Pearson, I. D. Brown and A. C. L. Mathieson, D. Reidel Publishing Co., Utrecht, 1962, vol. 27, p. 475.
- (a) D. C. Look, *Mater. Sci. Eng., B*, 2001, **80**, 383; (b) H.-M. Xiong, Z.-D. Wang, D.-P. Xie, L. Cheng and Y.-Y. Xia, *J. Mater. Chem.*, 2006, **16**, 1345; (c) S. C. Pillai, J. M. Kelly, D. E. McCormack and R. Ramesh, *J. Mater. Chem.*, 2004, **14**, 1572.
- K. Keis, L. Vayssiers, S. E. Lindquist and A. Hagfeldt, *Nanostruct. Mater.*, 1999, **12**, 487.
- T. Diet, H. Ohno, F. Matsukura, J. Gilbert and D. Ferrand, *Science*, 2000, **287**, 1019.
- For example, see: (a) N. S. Norberg, K. R. Kittilstved, J. E. Ammonette, R. K. Kukkadapu, D. A. Schwartz and D. R. Gamelin, *J. Am. Chem. Soc.*, 2004, **126**, 9387; (b) X. T. Zhang, Y. C. Liu, J. Y. Zhang, Y. M. Lu, D. Z. Shen, X. W. Fan and X. G. Kong, *J. Cryst. Growth*, 2003, **254**, 80; (c) C. N. R. Rao and F. L. Deepak, *J. Mater. Chem.*, 2005, **15**, 573; (d) K. Ueda, H. Tabata and T. Kawai, *Appl. Phys. Lett.*, 2001, **79**, 988.
- J. Schrier, D. O. Demchenko, L.-W. Wang and A. P. Alivisatos, *Nano Lett.*, 2007, **7**, 2377.
- C. Tsakonas and C. B. Thomas, *J. Appl. Phys.*, 1995, **78**, 6098.
- Y. P. Leung, C. H. W. Choy, I. Markov, G. K. H. Pang, H. C. Ong and T. I. Yuk, *Appl. Phys. Lett.*, 2006, **88**, 183110.
- A. Erlacher, A. R. Lukaszew, H. Jaeger and B. Ullrich, *Surf. Sci.*, 2006, **600**, 3762.
- N. Brilis, P. Romesis, D. Tsamakis and M. Kompitsas, *Superlattices Microstruct.*, 2005, **38**, 283.
- H. Cheng, J. Cheng, Y. Zhang and Q.-M. Wang, *J. Cryst. Growth*, 2007, **299**, 34.
- H. M. Manasevit and W. I. Simpson, *J. Electrochem. Soc.*, 1971, **118**, 644.
- B. Cockayne, P. J. Wright, A. J. Armstrong, A. C. Jones and E. D. Orrell, *J. Cryst. Growth*, 1988, **91**, 57.
- P. J. Wright, P. J. Parbrook, B. Cockayne, A. C. Jones, E. D. Orrell, K. P. O'Donnell and B. Henderson, *J. Cryst. Growth*, 1989, **94**, 441.
- O. F. Z. Khan, P. O'Brien, P. A. Hamilton, J. R. Walsh and A. C. Jones, *Chemtronics*, 1989, **4**, 224.
- C. L. Griffiths, A. Stafford, S. J. Irvine, N. Maung, A. C. Jones, L. M. Smith and S. A. Rushworth, *Appl. Phys. Lett.*, 1996, **68**, 1294.
- S. J. Bass and P. E. Oliver, *GaAs and Related Compounds*, Conf. Ser. 33b, Inst. Physics, London, 1977, p. 1.
- R. W. Glew, *J. Cryst. Growth*, 1984, **68**, 44.
- V. Aebi, C. B. Cooper, R. L. Moon and R. R. Saxena, *J. Cryst. Growth*, 1981, **55**, 517.
- A. C. Jones, S. A. Rushworth, P. O'Brien, J. R. Walsh and C. Meaton, *J. Cryst. Growth*, 1993, **130**, 295.
- P. O'Brien, in *Inorganic Materials*, ed. D. Bruce, and D. O'Hare, Wiley, Chichester, 1997, p. 523.
- I. G. Dance, R. G. Garbutt, D. C. Craig and M. L. Scudder, *Inorg. Chem.*, 1987, **26**, 3732.
- I. G. Dance, R. G. Garbutt, D. C. Craig and M. L. Scudder, *Inorg. Chem.*, 1987, **26**, 4057.
- I. G. Dance, R. G. Garbutt and M. L. Scudder, *Inorg. Chem.*, 1990, **29**, 1571.
- M. B. Hursthouse, O. F. Z. Khan, M. Mazid, M. Motevalli and P. O'Brien, *Polyhedron*, 1990, **9**, 541.
- O. F. Z. Khan and P. O'Brien, *Polyhedron*, 1991, **10**, 325.
- M. Bochmann, K. J. Webb, M. Harman and M. B. Hursthouse, *Angew. Chem., Int. Ed. Engl.*, 1990, **29**, 638.
- M. Bochmann, K. J. Webb, M. B. Hursthouse and M. Mazid, *J. Chem. Soc., Dalton Trans.*, 1991, 2317.
- M. Bochmann and K. J. Webb, *J. Chem. Soc., Dalton Trans.*, 1991, 2325.
- B. O. Dabbousi, P. J. Bonasia and J. Arnold, *J. Am. Chem. Soc.*, 1991, **113**, 3186.
- P. J. Bonasia and J. Arnold, *Inorg. Chem.*, 1992, **31**, 2508.
- J. Arnold, J. M. Walker, K. M. Yu, P. J. Bonasia, A. L. Seligson and E. D. Bourret, *J. Cryst. Growth*, 1992, **124**, 647.
- Y. Takahashi, R. Yuki, M. Segiura, S. Motojima and K. Sugiyama, *J. Cryst. Growth*, 1980, **50**, 491.
- R. D. Pike, H. Cui, R. Kershaw, K. Dwight, A. Wold, T. N. Blanton, A. A. Wernberg and H. J. Gysling, *Thin Solid Films*, 1993, **224**, 221.
- M. B. Hursthouse, M. A. Malik, M. Motevalli and P. O'Brien, *Polyhedron*, 1992, **11**, 45.
- M. A. Malik and P. O'Brien, *Adv. Mater. Opt. Electron.*, 1994, **3**, 171.
- M. B. Hursthouse, M. A. Malik, M. Motevalli and P. O'Brien, *J. Mater. Chem.*, 1992, **9**, 949.
- M. Chunggaze, J. McAleese, P. O'Brien and D. J. Otway, *Chem. Commun.*, 1998, 833.
- G. Barone, T. Chaplin, T. G. Hibbert, A. T. Kana, M. F. Mahon, K. C. Molloy, I. D. Worsley, I. P. Parkin and L. S. Price, *J. Chem. Soc., Dalton Trans.*, 2002, 1085.
- (a) L. H. Van Poppel, T. H. Groy and M. T. Caudle, *Inorg. Chem.*, 2004, **43**, 3180; (b) A. A. Memon, M. Afzaal, M. A. Malik, C. Q. Nguyen, P. O'Brien and J. Raftery, *Dalton Trans.*, 2006, 4489.
- M. Afzaal, S. M. Aucott, D. Crouch, P. O'Brien, J. D. Woollins and J.-H. Park, *Chem. Vap. Deposition*, 2002, **8**, 187.
- M. Afzaal, D. Crouch, M. A. Malik, M. Motevalli, P. O'Brien, J.-H. Park and J. D. Woollins, *Eur. J. Inorg. Chem.*, 2004, 171.
- G. G. Briand, T. Chivers and M. Parvez, *Angew. Chem., Int. Ed.*, 2002, **41**, 3468.
- T. Chivers, D. J. Eisler and J. S. Ritch, *Dalton Trans.*, 2005, 2675.

- 62 S. S. Garje, J. S. Ritch, D. J. Eisler, M. Afzaal, P. O'Brien and T. Chivers, *J. Mater. Chem.*, 2006, **16**, 966.
- 63 J. S. Ritch, T. Chivers, M. Afzaal and P. O'Brien, *Chem. Soc. Rev.*, 2007, **36**, 1622.
- 64 K. Govender, D. S. Boyle, P. B. Kenway and P. O'Brien, *J. Mater. Chem.*, 2004, **14**, 2575.
- 65 (a) Y. F. Chen, D. M. Bagnall and T. Yao, *Mater. Sci. Eng., B*, 2000, **75**, 190; (b) X. Fang and L. Zhang, *J. Mater. Sci. Technol.*, 2006, **22**, 1.
- 66 (a) A. Chittofrati and E. Matijevic, *Colloids Surf.*, 1990, **48**, 65; (b) P. Yang, H. Yan, S. Mao, R. Russo, J. Hohnson, R. Saykally, N. Morris, J. Pham, R. He and J.-H. Choi, *Adv. Funct. Mater.*, 2002, **12**, 323.
- 67 R. A. McBride, J. M. Kelly and D. E. McCormack, *J. Mater. Chem.*, 2003, **13**, 1196.
- 68 K. Fujita, K. Murata, T. Nakazawa and I. Kayama, *Yogyo Kyokaiishi*, 1984, **92**, 227.
- 69 L. Vayssieres, K. Keis, S. T. Lindquist and A. Hagfeldt, *J. Phys. Chem. B*, 2001, **105**, 3350.
- 70 T. Dedova, M. Krunk, A. Mere, J. Klauson and O. Volobueva, *Mater. Res. Soc.*, 2007, **957**, 359.
- 71 D. S. Boyle, K. Govender and P. O'Brien, *Chem. Commun.*, 2002, 80.
- 72 D. S. Boyle, K. Govender, D. Binks, D. West, D. Coleman and P. O'Brien, *Adv. Mater.*, 2002, **14**, 1221.
- 73 M. Andrés-Vergés, A. Mifsud and C. J. Serna, *J. Chem. Soc., Faraday Trans.*, 1990, **86**, 959.
- 74 J. Zhang, L. Sun, J. Yin, H. Su, C. Liao and C. Yan, *Chem. Mater.*, 2002, **14**, 4172.
- 75 (a) A. M. Peiro, P. Ravirajan, K. Govender, D. S. Boyle, P. O'Brien, D. D. C. Bradley, J. Nelson and J. R. Durrant, *J. Mater. Chem.*, 2006, **16**, 2088; (b) J. H. Xiang, P. X. Zhu, Y. Masuda, M. Okuya, S. Kaneko and K. Koumoto, *J. Sci. Nanotechnol.*, 2006, **6**, 1797.
- 76 A. Pudov, J. Sites and T. Nakada, *Jpn. J. Appl. Phys.*, 2002, **41**, L672.
- 77 A. Bayer, D. S. Boyle and P. O'Brien, *J. Mater. Chem.*, 2002, **12**, 2940.
- 78 B. Mokili, M. froment and D. Lincot, *J. Phys. III*, 1995, **5**, C3261.
- 79 P. O'Brien and J. McAleese, *J. Mater. Chem.*, 1998, **8**, 2309.
- 80 I. C. Ndukwe, *Sol. Energy Mater. Sol. Cells*, 1996, **40**, 123.
- 81 B. Mokili, Y. Charreire, R. Cortes and D. Lincot, *Thin Solid Films*, 1996, **288**, 21.
- 82 I. O. Oladeji and I. Chow, *Thin Solid Films*, 1999, **339**, 148.
- 83 J. Lee, S. Lee, S. Cho, S. Kim, I. Y. Park and Y. D. Choi, *Mater. Chem. Phys.*, 2002, **77**, 254.
- 84 D. Lincot and R. Ortega-Borges, *J. Electrochem. Soc.*, 1992, **139**, 1880.
- 85 J. M. Dona and J. Herrero, *J. Electrochem. Soc.*, 1994, **141**, 205.
- 86 R. Ortega-Borges, D. Lincot and J. Vedel, in *Proceedings of the 11th E. C. Photovoltaic Solar Energy Conference*, Harwood Academic Publishers, Switzerland, 1992, p. 862.
- 87 D. S. Boyle, O. Robbe, D. P. Halliday, M. R. Heinrich, A. Bayer, P. O'Brien, D. J. Otway and M. D. G. Potter, *J. Mater. Chem.*, 2000, **10**, 2439.
- 88 C. N. R. Rao, G. U. Kulkarni, P. J. Thomas, V. V. Agrawal and P. Saravanan, *J. Phys. Chem. B*, 2003, **107**, 7391.
- 89 C. N. R. Rao, G. U. Kulkarni, V. V. Agrawal, U. K. Gautam, M. Ghosh and U. Tumkurkar, *J. Colloid Interface Sci.*, 2005, **289**, 305.
- 90 P. J. Thomas, D. Fan and P. O'Brien, *J. Nanosci. Nanotechnol.*, 2007, **7**, 1689.
- 91 U. K. Gautam, M. Ghosh and C. N. R. Rao, *Langmuir*, 2004, **20**, 10775.
- 92 (a) K. P. Kalyanikutty, U. K. Gautam and C. N. R. Rao, *Solid State Sci.*, 2006, **8**, 296; (b) C. N. R. Rao, S. R. C. Vivekchand, K. Biswasa and A. Govindaraja, *Dalton Trans.*, 2007, 3728.
- 93 D. Fan, P. J. Thomas and P. O'Brien, *J. Mater. Chem.*, 2007, **27**, 1381.
- 94 T. Trindade, P. O'Brien and N. L. Pickett, *Chem. Mater.*, 2001, **13**, 3843.
- 95 N. S. Pesika, Z. Hu, K. J. Stebe and P. C. Searson, *J. Phys. Chem. B*, 2002, **106**, 6985.
- 96 L. Spanhel and M. A. Anderson, *J. Am. Chem. Soc.*, 1991, **113**, 2826.
- 97 L. Guo, Y. L. Ji, H. B. Xu, P. Simon and Z. Y. Wu, *J. Am. Chem. Soc.*, 2002, **124**, 14864.
- 98 U. Koch, A. Fojtik, H. Weller and A. Henglein, *Chem. Phys. Lett.*, 1985, **122**, 507.
- 99 E. A. Muelenkamp, *J. Phys. Chem. B*, 1998, **102**, 5566.
- 100 A. Wood, M. Giersig, M. Hilgendorff, A. Vilas-Campos, L. M. Liz-Marzan and P. Mulvaney, *Aust. J. Chem.*, 2003, **56**, 1051.
- 101 H. Zhou, H. Alves, D. M. Hofmann, W. Kriegseis, B. K. Meyer, G. Kaczmarczyk and A. Hoffmann, *Appl. Phys. Lett.*, 2002, **80**, 210.
- 102 A. V. Dijken, E. A. Meulenkamp, D. Vanmaekelbergh and A. Meijerink, *J. Lumin.*, 2000, **90**, 123.
- 103 M. Shim and P. Guyot-Sionnest, *J. Am. Chem. Soc.*, 2001, **123**, 11651.
- 104 P. D. Cozzoli, M. L. Curri, A. Agostiano, G. Leo and M. Lomascolo, *J. Phys. Chem. B*, 2003, **107**, 4756.
- 105 C. G. Kim, K. Sung, T.-M. Chung, D. Y. Jung and Y. Kim, *Chem. Commun.*, 2003, 2068.
- 106 J. Hambrock, S. Rabe, K. Merz, A. Birkner, A. Wohlfart, R. A. Fischer and M. Driess, *J. Mater. Chem.*, 2003, **13**, 1731.
- 107 T. Andelman, Y. Gong, M. Polking, M. Yin, I. Kuskovsky, G. Neumark and S. O'Brien, *J. Phys. Chem. B*, 2005, **109**, 14314.
- 108 Y. Chen, M. Kim, G. Lian, M. B. Johnson and X. Peng, *J. Am. Chem. Soc.*, 2005, **127**, 13331.
- 109 N. S. Norberg and D. R. Gamelin, *J. Phys. Chem. B*, 2005, **109**, 20810.
- 110 Y. S. Wang, P. J. Thomas and P. O'Brien, *J. Phys. Chem. B*, 2006, **110**, 4099.
- 111 T. Dietl, H. Ohno, F. Matsukura, J. Gilbert and D. Ferrand, *Science*, 2000, **287**, 1019.
- 112 N. S. Norberg, K. R. Kittilstved, J. E. Amonette, R. K. Kukkadapu, D. A. Schwartz and D. R. Gamelin, *J. Am. Chem. Soc.*, 2004, **126**, 9387.
- 113 X. T. Zhang, Y. C. Liu, J. Y. Zhang, Y. M. Lu, D. Z. Shen, X. W. Fan and X. G. Kong, *J. Cryst. Growth*, 2003, **254**, 80.
- 114 C. N. R. Rao and F. L. Deepak, *J. Mater. Chem.*, 2005, **15**, 573.
- 115 K. Ueda, H. Tabata and T. Kawai, *Appl. Phys. Lett.*, 2001, **79**, 988.
- 116 M. Liu, A. H. Kitai and P. Mascher, *J. Lumin.*, 1992, **54**, 35.
- 117 T. Fukumura, Z. W. Jin, A. Ohtomo, H. Koinuma and M. Kawasaki, *Appl. Phys. Lett.*, 1999, **75**, 3367.
- 118 Z. W. Jin, Y. Z. Yoo, T. Sekiguchi, T. Chikyow, H. Ofuchi, H. Fujioka, M. Oshima and H. Koinuma, *Appl. Phys. Lett.*, 2003, **83**, 3367.
- 119 C.-H. Ku, H.-H. Chiang and J. J. Wu, *Chem. Phys. Lett.*, 2005, **404**, 132.
- 120 A. Y. Polyakov, A. V. Govorkov, N. B. Smirnov, N. V. Pashkova, S. J. Pearton, K. I. R. M. Frazier, C. R. Abernathy, D. P. Norton, J. M. Zavada and R. G. Wilson, *Mater. Sci. Semicond. Process.*, 2004, **7**, 77.
- 121 S. C. Erwin, L. Zu, M. I. Haftel, A. L. Efros, T. Kennedy and D. J. Norris, *Nature*, 2005, **436**, 91.
- 122 Y. S. Wang, P. J. Thomas and P. O'Brien, *J. Phys. Chem. B*, 2006, **110**, 21412.
- 123 A. Henglein, *Chem. Rev.*, 1989, **89**, 1861.
- 124 M. L. Steigerwald and L. E. Brus, *Acc. Chem. Res.*, 1990, **23**, 183.
- 125 M. G. Bawendi, M. L. Steigerwald and L. E. Brus, *Annu. Rev. Phys. Chem.*, 1990, **41**, 477.
- 126 H. Weller, *Angew. Chem., Int. Ed. Engl.*, 1993, **32**, 41.
- 127 H. Weller, *Adv. Mater.*, 1993, **5**, 88.
- 128 A. Hagfeldt and M. Grätzel, *Chem. Rev.*, 1995, **95**, 49.
- 129 J. H. Fendler and F. C. Meldrum, *Adv. Mater.*, 1995, **7**, 607.
- 130 A. P. Alivisatos, *J. Phys. Chem.*, 1996, **100**, 13226.
- 131 R. J. Hunter, *Introduction to Modern Colloid Science*, Oxford University Press, Oxford, UK, 1993.
- 132 D. M. Whelmy and E. J. Matijevic, *J. Chem. Soc., Faraday Trans. 1*, 1984, **80**, 563.
- 133 C. B. Murray, D. J. Norris and M. G. Bawendi, *J. Am. Chem. Soc.*, 1993, **115**, 8706.
- 134 M. A. Hines and P. Guyot-Sionnest, *J. Phys. Chem. B*, 1998, **102**, 3665.

- 135 N. L. Pickett and P. O'Brien, *Chem. Rec.*, 2001, **1**, 467.
- 136 M. A. Malik, P. O'Brien and N. Revaprasadu, *Chem. Mater.*, 2002, **14**, 2004.
- 137 N. Revaprasadu, M. A. Malik, P. O'Brien and G. Wakefield, *J. Mater. Res.*, 1999, **14**, 3237.
- 138 B. Ludolph, M. A. Malik, P. O'Brien and N. Revaprasadu, *Chem. Commun.*, 1998, 1849.
- 139 (a) Y.-W. Jun, J.-E. Koo and J. Cheon, *Chem. Commun.*, 2000, 1243; (b) Y.-W. Jun, C.-S. Choi and J. Cheon, *Chem. Commun.*, 2001, 101.
- 140 M. D. Nyman, M. J. Hampden-Smith and E. N. Duesler, *Inorg. Chem.*, 1997, **36**, 2218.
- 141 S. L. Cumberland, K. M. Hanif, A. Javier, K. A. Khitov, G. F. Strouse, S. M. Woessner and C. S. Yun, *Chem. Mater.*, 2002, **14**, 1576.
- 142 M. W. DeGroot, C. Khadka, H. Rösner and J. F. Corrigan, *J. Cluster Sci.*, 2006, **17**, 97.
- 143 Y. Li, X. Li, C. Yang and Y. Li, *J. Phys. Chem. B*, 2004, **108**, 16002.
- 144 C. Q. Nguyen, A. Adeogun, M. Afzaal, M. A. Malik and P. O'Brien, *Chem. Commun.*, 2006, 2179.
- 145 C. Q. Nguyen, M. Afzaal, M. A. Malik, M. Helliwell, J. Raftery and P. O'Brien, *J. Organomet. Chem.*, 2007, **692**, 2669.
- 146 M. W. DeGroot, H. Rösner and J. F. Corrigan, *Chem.-Eur. J.*, 2006, **12**, 1547.
- 147 (a) C. M. Niemeyer and C. A. Mirkin, *Nanobiotechnology: Concepts, Applications and Perspectives*, Wiley-VCH, Weinheim, 2004; (b) J. Wang, *Small*, 2005, **1**, 1036.
- 148 (a) R. Weissleder, K. Kelly, E. Y. Sun, T. Shtatland and L. Josephson, *Nat. Biotechnol.*, 2005, **23**, 1418; (b) J. W. M. Bulte, S. C. Zhang, P. Van Gelderen, V. Herynek, E. K. Jordan, I. D. Duncan and J. A. Frank, *Proc. Natl. Acad. Sci. U. S. A.*, 1999, **96**, 15256; (c) Y. W. Jun, Y. M. Huh, J. S. Choi, J. H. Lee, H. T. Song, S. Kim, S. Yoon, K. S. Kim, J. S. Shin, J. S. Suh and J. Cheon, *J. Am. Chem. Soc.*, 2005, **127**, 5732; (d) J. Won, M. Kim, Y. W. Yi, Y. H. Kim, N. Jung and T. K. Kim, *Science*, 2005, **309**, 121; (e) J. Park, J. Joo, S. G. Kwon, Y. Jang and T. Hyeon, *Angew. Chem., Int. Ed.*, 2007, **46**, 4630; (f) H. Gu, P. L. Ho, K. W. T. Tsang, L. Wang and B. Xu, *J. Am. Chem. Soc.*, 2003, **125**, 15702; (g) N. R. Jana, H.-H. Yu, E. M. Ali, Y. Zheng and J. Y. Ying, *Chem. Commun.*, 2007, 1406.
- 149 (a) J. J. Urban, D. V. Talapin, E. V. Shevchenko and C. B. Murray, *J. Am. Chem. Soc.*, 2006, **128**, 3248; (b) E. V. Shevchenko, D. V. Talapin, C. B. Murray and S. O'Brien, *J. Am. Chem. Soc.*, 2006, **128**, 3620; (c) E. V. Shevchenko, D. V. Talapin, S. O'Brien and C. B. Murray, *J. Am. Chem. Soc.*, 2005, **127**, 8741; (d) F. X. Redl, K.-S. Cho, C. B. Murray and S. O'Brien, *Nature*, 2003, **423**, 968; (e) A. Courty, C. Fermon and M. P. Pileni, *Adv. Mater.*, 2001, **13**, 254; (f) A. Courty, A. Mermet, P. A. Albouy, E. Duval and M. P. Pileni, *Nat. Mater.*, 2005, **4**, 395; (g) E. V. Shevchenko, D. V. Talapin, N. A. Kotov, S. O'Brien and C. B. Murray, *Nature*, 2006, **439**, 55; (h) Y. Xia, P. Yang, Y. sun, Y. Wu, B. Mayers, B. Gates, Y. Yin, F. Kim and H. Yan, *Adv. Mater.*, 2003, **15**, 353.